

Sub-ambient CO oxidation over Au/MO_x/CeO₂- Al₂O₃ (M=Zn or Fe)

Tomás Ramírez Reina, Svetlana Ivanova*, María Isabel Domínguez, Miguel Angel Centeno, José Antonio Odriozola

Instituto de Ciencia de Materiales de Sevilla, Centro mixto CSIC-Universidad de Sevilla,
Avda. Américo Vespucio 49, 41092 Sevilla, Spain

*svetlana@icmse.csic.es

Abstract

A series of ZnO and Fe₂O₃ modified ceria/alumina supports and their corresponding gold catalyst were prepared and studied in the CO oxidation reaction. ZnO-doped solids show a superior catalytic activity compared to the bare CeO₂-Al₂O₃, this is attributed to the intimate contact of the ZnO and CeO₂ phases since an exchange of the lattice oxygen occurs at the interface. In a similar way, Fe₂O₃-modified supports enhanced the ability of the CeO₂-Al₂O₃ solids to eliminate CO till the phase segregation occurs, an effect strictly dependent on the Fe₂O₃ loading. Concerning the gold catalysts, all of them were very efficient in the oxidation of CO no matter the doping metal oxide or loading, with the ZnO containing systems better than the others. The majority of the systems reached total CO conversion below room temperature being the ZnO and Fe₂O₃ monolayer loaded systems the most efficient within the series.

Keywords: gold catalyst, zinc oxide, iron oxide, monolayer, CO oxidation.

Introduction

In the last 20 years gold based catalysis received a very special attention in the scientific community. The surprising discovery of Haruta et al. [1] that very small gold nanoparticles exhibit catalytic activity for the oxidation of CO at sub-ambient temperature provokes an enormous scientific interest and makes gold the most used and the most popular metal for CO catalytic oxidation reaction. There are really a vast number of publications on this subject, several reviews and a book which try to unite the biggest part of information [2-5]. Nevertheless the diversity of the catalytic system or employed oxidation reactions, everybody agreed on the importance paid to the nature of the active phase-gold particle size and structural geometry (existence of defect sites), to the nature of support and its interactions with gold, to the pre-reactional treatment and/or reaction conditions (especially presence of moisture). A general drawback of the gold nanoparticles is the fact that they are kinetically unstable and have higher tendencies for agglomeration in high temperature applications. However, the thermal stability could be improved by a careful choice of the support material, which first role is to disperse and stabilize the nanoparticles against agglomeration.

CeO₂ has been broadly reported as an active support for oxidation catalyst due to its chemical properties [6-9]. As mentioned above, the principal role of the support is to stabilize and disperse the metal particles, and for this a high specific surface area is required in order to provide a strong metal-support interaction. Lower the support crystallites are, better the dispersion of the metal particles and lower their size [10]. It was reported by Andreeva et al. [11] that the addition of Al₂O₃ to CeO₂, as a textural promoter prevents the sinterization of CeO₂ crystallites and avoids the agglomeration of the Au during the WGS reaction thus maintaining a high catalytic activity in the steady state.

In addition, ceria is very useful in the oxidation reactions due to its redox behaviour, allowing oxygen mobility, and enhancing the oxygen exchange with the medium. Another feature of this support, which should be taken into consideration, is that ceria is an n-type semiconductor whose band structure can be modified by promoters. Several studies have demonstrated that doping of CeO₂ with elements with different ionic radii and oxidation state improves the exchange of oxygen in the oxide network by decreasing the energy barrier for oxygen migration [12-15]. Iron is an interesting dopant, especially because of its own redox behaviour (Fe³⁺/Fe²⁺). Zn as well has been used as a CeO₂-doping metal and a positive effect of its addition on the catalytic performance have been reported [16]. However, Ce-Zn solid solution formation has not been reported, being the interface (or the perimeter of contact) between ZnO and CeO₂ the region where a strong Zn-O-Ce interaction is produced.

In gold based catalysis not only the high activity matters, but also the stability of the system under operating conditions. It is likely, that the intimate interaction between gold and the support is crucial for the high performance. Fu et al. [17] have reported that the loss of activity could be due to the loss of surface area of the ceria support due to weakening of the Au/ceria interaction. In this context, supporting ceria on a high surface area oxide carrier should be a good solution to the problem of ceria crystallites sintering and loss of activity. Moreover, any addition of doping metal with or without formation of the solid solution or epitaxial growth will promote the oxygen mobility of the ceria thus facilitating the oxygen exchange with the reaction media.

Nieuwenhuys et al. [18-21] reported that the addition of metal oxides to Au/Al₂O₃ can significantly improve the catalytic activity at low temperature CO oxidation applications. They described a model in which the reaction solely takes places at the

Au/MO_x perimeter with the CO adsorbed on Au and the MO_x acting as a supplier of oxygen. They report multicomponent catalysts comprising transition metal oxide and alkali oxides but do not consider the combination of one transition metal oxide and one rare earth oxide.

In this scenario, the aim of this work is to study the effect of the presence of transition metal oxides (ZnO or Fe₂O₃) on the CeO₂-Al₂O₃ electronic properties and on its activity and stability in CO oxidation reactions before and after gold deposition. Both oxides were chosen in order to have one “irreducible” oxide (ZnO) and one “reducible” oxide with its own redox couple (Fe³⁺/Fe²⁺).

Experimental

Synthesis of the supports

The supports were synthesized by conventional impregnation of doping metal oxide on a commercial CeO₂-Al₂O₃ support (Puralox, Sasol). The necessary amounts of metal precursor (zinc nitrate or iron nitrate, Aldrich) were impregnated in ethanolic solution in order to obtain 0.5, 1 and 1.5 theoretical monolayers of metal doping oxide on CeO₂-Al₂O₃ support. The as prepared supports were then calcined at 500 °C during 4 hours.

The calculation of the layer coverage was made under assumption that ZnO will expose its hexagonal base on the surface of the CeO₂-Al₂O₃ support and this base is occupied by only one ZnO molecule. The same supposition is made for the Fe₂O₃ hematite structure with the only difference of exposing its square base of the rhombohedral lattice. The space groups of the both oxides and the calculations of the monolayer are presented in Figure 1.

Figure 1

Gold deposition

The gold deposition (2 wt% nominal loading) was performed by the direct anionic exchange method, assisted by NH_3 (30 % Aldrich) as described elsewhere [22]. The obtained solids were dried overnight at 70°C and finally calcined at 400°C during 2 h with a heating rate of $10^\circ\text{C}\cdot\text{min}^{-1}$. In the adopted nomenclature, the MO_x contents are expressed as a number of theoretical monolayers over the commercial support. For example, the Au/0.5ZnO/CeAl solid contains the corresponding Au loading over half monolayer of ZnO deposited on $\text{CeO}_2\text{-Al}_2\text{O}_3$ support (Puralox, Sasol).

Characterization

The chemical composition of the samples was determined by X-Ray microfluorescence spectrometry (XRMF) in an EDAX Eagle III spectrophotometer with a rhodium source of radiation.

The textural properties were studied by N_2 adsorption measurements at liquid nitrogen temperature. The experiments were carried out on Micromeritics ASAP 2010 equipment. Before analysis, the samples were degassed for 2 h at 150°C in vacuum. The Berrett-Joyner-Halenda (BJH) method was used for determining the pore size distributions, and in every case the desorption isotherm was used.

X-ray diffraction (XRD) analysis was performed on an X'Pert Pro PANalytical. Diffraction patterns were recorded with $\text{Cu K}\alpha$ radiation (40 mA, 45 kV) over a 2Θ -range of 10 to 80° and a position-sensitive detector using a step size of 0.05° and a step time of 80 s.

The Temperature Programmed Reduction (TPR) experiments were carried out in a conventional quartz reactor connected to a thermal conductivity detector (TCD). The reactive gas stream with a flow rate of $50 \text{ mL}\cdot\text{min}^{-1}$ was streamed through 50 mg of sample and the temperature rose at $10^\circ\text{C}\cdot\text{min}^{-1}$ from room temperature to 900°C . A molecular sieve 13X was used to retain the H_2O producing during the reduction and/or CO_2 which could be desorbed from the solid surface. For quantitative analysis the experimental consumption was compared to those of CuO (99.999 %) reference.

Catalytic activity

The activity measurements were carried out in a U-shape glass flow reactor at atmospheric pressure. The catalysts were pretreated in a 30 mL min^{-1} activation flow of 21% O_2 balanced in He (from room temperature to 400°C , 5°C min^{-1}). After the activation a reactive flow (3.4% CO and 21% O_2 , balanced by helium) was passed through the reactor at room temperature. The gas total flow was 42 mL min^{-1} and the quantitative analysis was carried out with a Blazers Omnistar Bentchop mass spectrometer. The catalysts were tested in the reaction flow at room temperature until reached the steady state. Then, the systems were heated to 400°C at $5^\circ\text{C}/\text{min}^{-1}$. To study in details the catalysts behaviour as a function of MO_x -content the same reaction was carried out at temperatures below 0°C . The reactor, loaded with a fresh and activated sample, was immersed into a cooling bath composed by liquid N_2 and acetone. Once the temperature stabilized, the reactive flow described above was flushed through the reactor. The temperature was increased slowly to the room temperature and the quantitative analysis of the reactives and products was carried out on a Blazers Omnistar Bentchop mass spectrometer.

Results and discussion

Chemical compositions of the prepared solids are presented in Table 1. The calculated values, expressed in weight percent for the half, one, and one and a half theoretical monolayer of ZnO are respectively, 3.6 ,7.3 and 10.9 wt.%. Those for the Fe₂O₃ systems are 3.9, 7.9 and 11.8 wt%.

A number of points have to be taken into account, considering the highly basic media during the gold deposition. At first place, the integrity of the primary support CeO₂-Al₂O₃, for which no influence of the ammonia treatment on the CeO₂ content is observed. On the other hand, the ZnO and Al₂O₃ seem to dissolve a bit during the gold deposition. It should be mentioned, that the Au/1.5ZnO/CeAl shows higher loading in ZnO than the parent 1.5ZnO/CeAl which is caused probably by the higher degree of dissolution of the Al₂O₃. As for the gold loading, the obtained values are very close to the desired ones. Only a small gold loss was observed for the Au/1ZnO/CeAl sample.

As for the systems doped with Fe₂O₃ the ammonia treatment during the gold deposition appears to influence the Al₂O₃ content but not the Fe₂O₃ and CeO₂ loading. This observation is in agreement with the well known chemical nature of the used oxides, ZnO as an amphoteric oxide is more susceptible to dissolve in the basic solutions than the Fe₂O₃ oxide which is easily dissolved only in acid solutions.

However, for Fe₂O₃ doped systems a significant gold loss was detected, varying between 25 and 35%. Recently, it was reported [15, 16] that the utilization of ZnO as structural modifier promotes the creation of the preferential sites for gold deposition and dispersion, which could explain the higher degree of gold deposition on ZnO modified support compared to the Fe₂O₃ one.

No matter the doping metal, the one monolayer system showed poorer capacity to include gold in its composition which could be due to the stronger interaction doping oxide-support. This contact limits the ability to create new interactions with other species, gold particles in particular [23-25].

Concerning the textural properties, all the samples are mesoporous materials with pore sizes around 70 Å with specific surface area neighboring that of the primary support. No matter the doping transition metal oxide or the gold presence, the specific surface area seems to be governed by the primary support.

XRD patterns of the prepared ZnO doped supports are shown in Figure 2A. All the systems have diffractions similar to the bare support ($\text{CeO}_2\text{-Al}_2\text{O}_3$) (JCPDS# 48-0367 for $\gamma\text{-Al}_2\text{O}_3$ and JCPDS# 00-034-0394 for CeO_2). No signals due to the ZnO are present for the half monolayer sample due to the small amount of doping agent. It should be mentioned however, that the presence of $\gamma\text{-Al}_2\text{O}_3$ could masque the diffraction lines of any existing ZnO phase. Nevertheless, an increment in the most intense diffraction peak of ZnO ($2\theta = 56,5^\circ$), superimposed with that of the $\gamma\text{-Al}_2\text{O}_3$, and a very weak signal at around $2\theta \sim 62,8^\circ$ can be perceived for the ZnO loading above half monolayer indicating the formation of ZnO agglomerates on the surface.

Figure 2

A similar diffraction patterns are obtained for the Fe_2O_3 doped systems (Figure 2C). Again, all the systems present similar diffractions to the bare support - $\text{CeO}_2\text{-Al}_2\text{O}_3$ with no diffraction lines assigned to the Fe_2O_3 phase, (JCPDS# 00-033-0664). However, a higher amorphous character is observed for the samples containing Fe_2O_3 , which seems to be proportional to the Fe loading

XRD patterns of the prepared gold catalysts are shown in Figure 2B and 2D for the ZnO and Fe₂O₃ doped systems, respectively. All the systems manifest similar XRD diagrams corresponding to the primary support. In the case of the ZnO-doped systems, no changes in the XRD diagram of the corresponding support are observed. No signals due to gold are present. Thus, it can be concluded that ZnO presence stabilizes gold into a nanoparticle size, which **cannot** be detected by the XRD analysis. However, for the Fe₂O₃ doped systems the appearance of the gold metal diffractions (JCPDS# 4-0784) with the increase of Fe₂O₃ content is observed, indicating the increase of the gold particle size. It can be assumed, that the existence of small fractions of Fe²⁺ could help to reduce the gold precursor during its deposition and the subsequent calcinations procedure, thus presenting a negative effect on the gold nanoparticles size at higher Fe₂O₃ contents.

No matter the doping metal oxide no indications of solid oxide solution formation is observed. Neither broadening nor shifts could be observed in the main ceria diffraction peak. The systems seem to be composed by the primary support with finely dispersed metal oxide layer covering the support surface.

It is well known that the reducibility of the support may affect the catalyst and, as a consequence, its catalytic performance. The oxygen vacancies created during the reduction seems to improve the O₂ adsorption on the support and/or at the support– oxide interface, thus producing more active catalysts [26]. The TPR-H₂ profiles of the studied ZnO and Fe₂O₃ support systems with or without gold presence compared to the bare commercial (CeO₂-Al₂O₃) support are presented in Figure 3 and 4, respectively.

Figure 3 and 4

The original support $\text{CeO}_2\text{-Al}_2\text{O}_3$ shows two steps of reduction. The low temperature reduction peak at around 500°C attributed to the surface ceria reduction and the high temperature one at around 770°C assigned to the bulk reduction of Ce^{4+} to Ce^{3+} [27-29]. The deposition of only a half monolayer of ZnO decreases the temperature of reduction, starting at temperatures as low as 150°C . An additional effect is the narrowing of the first reduction peak. The increase of the ZnO content (deposition of one and one and a half monolayers of ZnO) intensifies the tendency of narrowing the superficial ceria reduction peak and the decrease of the temperature for ceria reduction.

The same observation was made for the Fe_2O_3 doped systems. Additionally, to the decrease of the temperature of the ceria reduction promoted by the presence of the Fe_2O_3 , supplementary reduction of the Fe_2O_3 can be observed. Wimmers et al. [30] studied the reduction of Fe_2O_3 and proposed a reduction in two steps $\text{Fe}_2\text{O}_3 \rightarrow \text{Fe}_3\text{O}_4 \rightarrow \text{Fe}$, with no formation of FeO . For the same oxide, other authors proposed a three steps reduction process considering FeO formation dealing with: $\text{Fe}_2\text{O}_3 \rightarrow \text{Fe}_3\text{O}_4$ at about 400°C , $\text{Fe}_3\text{O}_4 \rightarrow \text{FeO}$ at about 600°C and finally $\text{FeO} \rightarrow \text{Fe}$ at higher temperatures [31-34]. No matter the number of reduction steps of the Fe_2O_3 the separation of its reduction from that of the CeO_2 overlapping reduction zones is hard to obtain, but one can observe better separation of the reduction processes with the increase of the Fe_2O_3 content.

As for the gold containing systems, as expected the presence of gold decreases the temperature of reduction by facilitating the mobility of the H_2 molecule on the surface of the solid. It was reported earlier [7, 17] a shift in the reduction peaks related to the surface oxygen of CeO_2 in the presence of gold at much lower temperatures. For the ZnO doped solids the presence of gold diminishes the temperature of the first zone of reduction more

than 200°C. The high temperature reduction however is less affected, occurring at the same temperatures. Apart from this shift to lower temperatures, it could be observed that the reduction process takes place in a narrower temperature range, which means that the homogeneity of the reduction process is improved.

For the Fe₂O₃ containing systems the presence of gold provokes an overlapping of all the reduction steps into the 200-500°C temperature range. Instead of the decrease of the temperature of reduction no significant change of the reduction behavior compared to the supports is observed.

To compare quantitatively the change in the reduction behavior of the support with the addition of the transition metal oxide, the reduction percentage (RP) of every system was calculated according to the following equation [16]:

$$RP = E_{HC}/T_{HC} \times 100;$$

Where T_{HC} is the theoretical hydrogen consumption (in moles) necessary for complete reduction of all reducible components of the corresponding sample and E_{HC} is the experimental hydrogen consumption measured during the TPR. For the RP calculation of the ZnO doped systems it was considered that the Ce and Zn are present in their maximum oxidation state (Ce⁴⁺ and Zn²⁺), and both reduces from Zn²⁺ to Zn⁰ and Ce⁴⁺ to Ce³⁺. For the calculation of the Fe₂O₃ doped system it was considered that the Ce and Fe are present in their maximum oxidation state (Ce⁴⁺ and Fe³⁺), that the Fe³⁺ completely reduces to Fe⁰ and that Ce⁴⁺ reduces only to Ce³⁺. When gold is present in the samples, its reduction is discarded, and considered that its full reduction from Au³⁺ to Au⁰ occurs during the

calcination of the samples. RP values as a function of the MO_x (M=Zn or Fe) coverage of the samples are presented in Figure 5.

Figure 5

It has been proposed in the literature [16] a mechanism of CeO₂ reduction in the presence of ZnO consisting in the formation of an oxygen vacancy in ZnO phase which further oxidizes by reducing the ceria phase. This mechanism supposed that an increase of the reduction degree with the presence of the ZnO is expected. However, comparing the RP value with that of the primary support the improvement of the reduction behavior is observed only for the sample referred as one monolayer sample. In this sample, due to the homogeneous ZnO layer deposition, an increase of the intimate contact between the ZnO and CeO₂ is expected, enhancing the fraction of Zn and Ce atoms sharing oxygen atoms from the network. These oxygen atoms, possess a distorted environment for which a tension in the surrounding bondings is created, thus generating superficial reactivity favoring the oxygen mobility.

The samples containing less or more than a monolayer of ZnO presents lower reduction degree indicating heterogeneity of the sample. One could consider zones where ZnO accumulates to form agglomerates, which became a physical barrier for the reduction of CeO₂ by diminishing the diffusion of H₂ through the material. The same was observed by Larese et al. for the Ce-Zr based systems [35]. This hypothesis is confirmed by the fact that the increasing of the ZnO loading to one and a half layer additionally lowers the RP value. Surprisingly, the addition of gold does not promote the reducibility in terms of reduction percentage for the sample with one monolayer of ZnO, on the contrary

diminishes, the reduction degree. The reduction seems to be governed by the ZnO layer, to which the gold presence do not exercise any influence. The role of gold appears to be only to increase the velocity of the reduction, thus diminishing the temperature of reduction, without increasing the ratio of the reduced species.

On the contrary, for the samples with ZnO loading different from one monolayer the increase of the RP values is observed. It appears that the gold presence promote the ZnO mobility on the samples and the formation of ZnO islands. The heterogeneity of these samples facilitates the direct contact between gold and ceria surface thus promoting both the reduction velocity and the reduction degree.

For the Fe₂O₃ doped system a decrease of the reduction degree with the increase of the Fe₂O₃ loading is observed. The reduction seems to be governed by the reduction of the Fe₂O₃. The increase of the Fe₂O₃ content could provoke agglomeration of the iron oxide particles which could change the mechanism of reduction of the later. It was reported by Wimmers et al. [30] that with increasing of the particle size the rate-determining step could change from nucleation (uniform internal reduction) to phase boundary reaction, i.e. chemical reaction at the Fe₃O₄/Fe metal interface, and/or diffusion through the Fe metal product layer. The formation of the protective layer of Fe metal could difficult the H₂ diffusion thus diminishing the accessibility to the inner CeO₂ layer, which could explain the decrease of its reduction degree with the increase of the thickness of the Fe₂O₃ layer. The presence of gold do not influence a lot the reduction degree of these systems, as no significant changes in the RP values are observed.

The CO light-off curves for the prepared supports are presented in Fig. 6 and the respective values of T₅₀ (the temperature for which a 50% of CO conversion is obtained) are shown in Table 2.

Figure 6

Table 2

The presence of ZnO improves the catalytic performance of the CeO₂-Al₂O₃ support. It exist a direct relationship between the T₅₀ and the number of ZnO monolayers. The CO oxidation activity as a function of ZnO content follows the order:

$$1.5\text{ZnO/CeAl} \geq 1 \text{ ZnO/CeAl} > 0.5\text{ZnO/CeAl} \geq \text{CeAl}$$

The similar behavior of the samples with one and one and a half monolayer of ZnO reveals that one monolayer of ZnO seems to be the optimum loading in terms of CO oxidation activity promotion. It is worth to be mentioned that ZnO doped supports reach total conversion of CO at 400 °C while the bare CeO₂-Al₂O₃ had a 44% of conversion as a maximum. The superior catalytic activity compared to the bare CeO₂-Al₂O₃ could be assigned to the intimate contact of the ZnO and CeO₂ phases at which interface an exchange of the lattice oxygen occurs thus promoting the oxidation activity.

For the Fe₂O₃ doped systems a better catalytic performance compared to the bare CeO₂-Al₂O₃ as well is observed. The CO oxidation activity follows the order:

$$0.5 \text{ Fe}_2\text{O}_3/\text{CeAl} > 1 \text{ Fe}_2\text{O}_3/\text{CeAl} > 1.5 \text{ Fe}_2\text{O}_3/\text{CeAl} > \text{CeAl}$$

Despite of the iron intrinsic activity [19-21], in this series of samples the increase of iron content seems to have a negative influence on the catalytic activity. It was reported for the FeO_x/CeO₂ solids [14] that an increase of the Fe₂O₃ content produce phase segregation within the material, thus diminishing the Ce-Fe contact, and as a consequence the activity in the CO oxidation reaction. However, the existence of Fe₂O₃ as a separate phase was not observed by XRD, but the high degree of amorphisation of the samples (Figure 2C)

indicates the presence of the low crystalline iron oxide on the surface of the samples, which could be responsible for the decrease of the Ce-Fe contact.

The catalytic activity of the corresponding gold catalysts is shown in Figure 7, and the respective temperatures of 50% CO conversion (T_{50}) are presented in Table 2. All the ZnO doped gold catalysts present better catalytic activity than the corresponding gold supported on $\text{CeO}_2\text{-Al}_2\text{O}_3$. Moreover, the improvement is proportional to the ZnO contents as the sub-ambient T_{50} values reveal.

Figure 7.

It should be mentioned, however, that all the systems are very active in the CO oxidation reaction, which supposes that gold particle size governs the reaction. It was reported [15] that the main role of the ZnO as doping oxide is to provide additional nucleation sites for gold nanoparticles deposition. The later, together with the enhanced oxygen mobility of the ZnO- CeO_2 interface could explain the better catalytic activity of the ZnO doped systems.

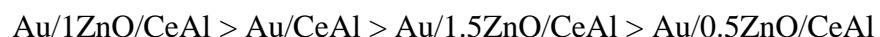
As for the gold supported Fe_2O_3 doped systems a negative effect with the iron oxide addition onto the $\text{CeO}_2\text{-Al}_2\text{O}_3$ oxide is observed. The lost of activity is proportional to the Fe_2O_3 content. As revealed by XRD, an increase of the gold particles size is observed for all those systems, which could explain the lower catalytic activity of the samples compared to gold supported on the primary support.

Several systems reach full conversion at room temperature and a study of the catalytic behaviour at sub-ambient temperature was carried out in order to distinguish better

the differences between the systems. The CO conversion as a function of the temperature for the corresponding gold containing systems is shown in Figure 8, and the respective values for T_{50} are presented in Table 2.

Figure 8

The obtained results for the ZnO doped systems in the sub-ambient CO oxidation reaction show a little bit different results, which in terms of activity has in the following order:



The best system appears to be the one monolayer ZnO promoted system. It is not surprising, in view of all discussed results, that the better ZnO to CeO₂ promotion in terms of oxide contact surface layer is observed. It was reported [36-38] that a monolayer or monomolecular dispersion of doping oxide is maximally influenced by the support. In addition the presence of one integral monolayer of ZnO without phase segregation or agglomeration is the optimal solution regarding the maximum nucleation sites available for the gold nanoparticles deposition. However, any contents below or under this value increase the possibility of a partial heterogeneity of the surface and/or lost of ZnO - CeO₂ contact surface, thus decreasing the CO oxidation activity. In such a way, the gold supported on the bare CeO₂ -Al₂O₃ support is more active than the half and one and a half ZnO layer promoted samples. Other interesting fact is that one monolayer ZnO promoted system has the lowest gold loading among the ZnO modified solids, but appears to be the most active.

As for the Fe₂O₃ doped systems, the catalytic activity at temperatures below 25°C changes dramatically. Again the gold supported on bare CeO₂ –Al₂O₃ support seems to be the more active, but this time is closely followed by the sample containing one monolayer of Fe₂O₃. As a general and very important observation, the Fe₂O₃ doped systems shows far better CO oxidation activity at sub-ambient temperature than when the reaction starts at 25°C. Complete CO conversion is achieved between 25 and 40°C for all the samples, excepting Au/1.5Fe₂O₃/CeAl. It was reported [39] that the gold dispersion could be improved by the redox mechanisms taking place between adsorbed CO on the gold species, ceria ions, and hydroxyl groups on the surface. At sub-ambient temperature the CO oxidation reaction is governed mainly by the CO adsorption onto gold particles surface. When the degree of adsorption (residence time of CO on gold metal surface) is increased the gold re-dispersion can occur thus providing more active sites at lower temperature and enhancing the catalytic activity. It is very important to mention, that this result shows that even the bigger size gold nanoparticles can be converted into a very active catalytic sites only with starting the CO oxidation reaction at sub-ambient temperatures. Here again the monolayer Fe₂O₃ doped sample shows an optimum activity, confirming that the better way to stabilize re-dispersed gold nanoparticles is to provide the possibility of maximum nucleation sites density. To confirm this hypothesis the XRD in the range 2θ 36-40° of the catalyst Au/1Fe₂O₃/CeAl before and after sub-ambient CO oxidation reaction was made (Figure 9).

Figure 9

As it is seen from the figure a decrease in the gold particle size takes place, being after the sub-ambient CO oxidation reaction, four times lower than for the fresh catalyst. The calculation of gold particle size by Scherrer equation on Au (111) diffraction line shows an average particle size decrease from 18 nm for the fresh catalyst to 5 nm after the CO oxidation, confirming the structural metal change, thus converting the catalyst in more active catalytic system.

Conclusions

It was demonstrated that the Zn-doped solids show a superior catalytic activity compared to the bare CeO₂-Al₂O₃ due to the intimate contact of the ZnO and CeO₂ phases at which interface an exchange of the lattice oxygen occurs.

The doping of the commercial support with iron oxide as well enhanced its ability to eliminate CO, an effect strictly dependent on the Fe₂O₃ loading, caused not only by the Fe₂O₃ intrinsic activity but by the phase separation and loss of the Ce-Fe contact surface.

Concerning the gold catalysts, in general, all the systems are very efficient in the oxidation of CO no matter the doping metal oxide or loading, with the ZnO containing systems better than the Fe₂O₃ ones.

At sub ambient temperature CO oxidation the modified systems with a monolayer of ZnO were the most efficient reaching total conversion at 5°C. However, the systems which dramatically change at low temperature are the Fe₂O₃ doped ones, for which gold re-dispersion occurs. The decrease of the gold particle size at around four times enhances the CO oxidation activity for these systems.

Finally, it can be concluded that for the both systems, ZnO or Fe₂O₃ promoted ones, the monolayer always shows an optimum activity, confirming that the better way to

stabilize and/or to re-disperse the gold nanoparticles is to provide the possibility of maximum nucleation sites density.

Acknowledgements

Financial support for this work has been obtained from the Spanish Ministerio de Ciencia e Innovación (ENE2009-14522-C05-01) cofinanced by FEDER funds from the European Union and from Junta de Andalucía (P09-TEP-5454). S. Ivanova acknowledges MEC for her contract Ramon y Cajal, Tomás Ramírez acknowledges CSIC for his JAE-Predoc fellowship and all the authors acknowledge Junta de Andalucía—“TEP 106 group”.

References

- [1] M. Haruta, T. Kobayashi, H. Sano, N. Yamada, *Chem. Lett.*, 1987, 2, 405.
- [2] G.C. Bond, D.T. Thompson, *Gold Bull.*, 2000, 33, 41.
- [3] M. Haruta, *Cattech*, 2002, 6, 102.
- [4] M.S. Chen, D.W. Goodman, *Catal. Today* 2006, 111, 22.
- [5] G. C. Bond, C. Louis, D. T. Thompson in *Catalysis by Gold*, (Ed. G. H. Hutchings) Imperial College Press, London, 2006.
- [6] A. Sandoval, A. Gomez-Cortés, R. Zanella, G. Diaz, J. M. Saniger, *J. Mol. Catal. A*, 2007, 278, 200.
- [7] G. Jacobs, E. Chenu, P.M. Patterson, L. Williams, D. Sparks, G. Thomas, B.H. Davis, *Appl. Catal. A* 258 (2004) 203.
- [8] M.A. Centeno, C. Portales, I. Carrizosa, J. A. Odriozola, *Cat. Lett.*, 2005, 102, 289.
- [9] S.-Y. Lai, Y. Qiu, S. Wang, *J. Catal.* 237 (2006) 303.
- [10] Carrettin S, Concepción P, Corma A, Nieto JML, Puentes VF, *Angewante Chemie-International Edition.*, 2004, 43, 2538.
- [11] Andreeva, D., Ivanov, I., Ilieva, L., Sobezak, J.W., Avdeev, G., Petrov, K. *Topics in Catalysis.*, 2007, 44 (1–2), 173.

- [12] W. Y. Hernández, M. A. Centeno, F. Romero-Sarria, J.A. Odriozola, *J.Phys. Chem. C.*, 2009, 113, 5629.
- [13] T. Tabakova, M. Manzoli, D. Paneva, F. Boccuzzi, V. Idakiev, I. Mitov, *Applied Catalysis B: Environmental* 101 (2011) 266–274.
- [14] O. H. Laguna, M. A. Centeno, G. Arzamendi, L. M. Gandía, F. Romero-Sarria, J. A. Odriozola., *Catalysis Today*, 2010, 157, 155.
- [15] O. H. Laguna, F. Romero-Sarria, M.A. Centeno, J.A. Odriozola, *J. Catal.*, 2010, 276, 360.
- [16] O.H. Laguna, M.A.Centeno, F. Romero-Sarria, J.A.Odriozola, 2011, *Catal. Today*, in press doi:10.1016/j.cattod.2011.02.015.
- [17] Fu, Q., Deng, W., Saltsburg, H., Flytzani-Stephanopoulos, M, *Appl. Catal.B: Env.*, 2005, 56, 57.
- [18] R.J.H Grisel, J.J. Slyconish, B.E. Nieuwenhuys, *Top. Catal.*, 2001, 16, 425.
- [19] R.J.H Grisel, B.E. Nieuwenhuys *Catal. Today*, 2001, 64, 69.
- [20] A.C. Gluhoi, M.A.P. Dekkers, B.E. Nieuwenhuys, *J. Catal.*, 2003, 219, 197
- [21] A.C. Gluhoi, B.E. Nieuwenhuys *Catal. Today*, 2007, 122, 226.
- [22] S. Ivanova, C. Petit, V. Pitchon, *Appl. Catal. A: Gen.*, 2004, 267, 191.
- [23] G.C. Bond, K. Brückman. *Faraday Disc. Chem Soc.*,1981, 72, 235.
- [24] F.Roozeboom, D.D. Cordingley, P.J. Gellins, *J.Catal.*,1981, 68, 464.

- [25] F.Roozeboom, A.J. Van Dillen, J.W. Geus, P.J. Gellins, *Ind. Eng. Chem. Prod. Res. Dev.*, 1981, 21, 304
- [26] D. Widmann, Y. Liu, F. Schüth, R.J. Behm, *J. Catal.*, 2010, 276, 292.
- [27] S.Damyanova, B.Pawelec, M.V.M. Huerta, J.L.G. Fierro, *Appl Catal. A:Gen.*, 2008, 337, 86.
- [28] D.Andreeva, V. Idakiev, T. Tabakova, L. Ilieva, P. Faralas, A. Bourlinos, A. Travlos, *Catal. Today*; 2002, 51
- [29] S.Y. Lai, Y.Qiu, S.Wang, *J. Catal.* 2006, 237, 303.
- [30] O. J. Wimmers, P. Arnoldy, J. A. Moulijn, *J. Phys. Chem.* 1986, 90, 1331.
- [31] L.I Ilieva, D.H. Andreeva, A.A. Andreev, *Thermochim. Acta.*, 1997, 292,
- [32] M. Khoudiakov, M.C. Gupta, S. Deevi, *Appl. Catal. A: Gen.*, 2005, 291, 151.
- [33] F.Bocuzzi, A. Chiorino, M- Manzoli, D. Andreeva, T. Tabakova, *J. Catal.*, 1999, 188, 39.
- [34] S.Paldey, S. Gedevanishvili, W.Zhang, F. Rasouli, *Appl. Catal. B: Env.*, 2005, 56, 241.
- [35] C. Larese, F.C. Galisteo, M. L. Granados, R. Mariscal, J.L.G. Fierro, P.S. Lambrou, A.M. Efstathiou, *J. Catal.* 226 (2004) 443-456.
- [36] A.J. Van Hengstum, J.G. Van Ommen, H. Bosch, P.J. Gellins, *Appl.Catal.*, 1983, 8, 369.

[37]] A.J. Van Hengstum, J.G. Van Ommen, J. Pranger, P.J. Gellins, *Appl. Catal.*,1984, 11, 369.

[38] I.E. Wachs, R.Y. Saleh, S.S. Chan, C.C. Chersich, *Appl. Catal.*,1985, 15, 339.

[39] F. Romero-Sarria, L. M. Martinez T., M. A. Centeno, J. A. Odriozola *J. Phys. Chem. C*, 2007, 111, 14469.